

A study of the nuclear medium influence on transverse momentum of hadrons produced in deep inelastic neutrino scattering

SKAT Collaboration

N.M. Agababyan¹, V.V. Ammosov², M. Atayan³,
N. Grigoryan³, H. Gulkanyan³, A.A. Ivanilov²,
Zh. Karamyan³, V.A. Korotkov²

¹ Joint Institute for Nuclear Research, Dubna, Russia

² Institute for High Energy Physics, Protvino, Russia

³ Yerevan Physics Institute, Armenia

YEREVAN 2003

Abstract

The influence of nuclear effects on the transverse momentum (p_T) distributions of neutrino-produced hadrons is investigated using the data obtained with SKAT propane-freon bubble chamber irradiated in the neutrino beam (with $E_\nu = 3\text{-}30$ GeV) at Serpukhov accelerator. Dependences of $\langle p_T^2 \rangle$ on the kinematical variables of inclusive deep-inelastic scattering and of the produced hadrons are measured. It has been observed, that the nuclear effects cause an enhancement of $\langle p_T^2 \rangle$ of hadrons (more pronounced for the positively charged ones) produced in the target fragmentation region at low invariant mass of the hadronic system ($2 < W < 4$ GeV) or at low energies transferred to the current quark ($2 < \nu < 9$ GeV). At higher W or ν , no influence of nuclear effects on $\langle p_T^2 \rangle$ is observed. Measurement results are compared with predictions of a simple model, incorporating secondary intranuclear interactions of hadrons (with a formation length extracted from the Lund fragmentation model), which qualitatively reproduces the main features of the data.

1 Introduction

The experimental study of the hadron production in deep inelastic scattering (DIS) of leptons on nuclei is an important source of information on the space-time evolution of the lepton-produced quark strings. Depending on the features of the latter, the nuclear medium influences differently the inclusive spectra of final hadrons, in particular, affecting their yields and the mean transverse momentum in various domains of the phase space. Hitherto no detailed data inferred in the same experiment are available for transverse momentum distributions in the lepton-nucleus DIS. This gap is partly filled by the present work, where the influence of the nuclear effects on the transverse momentum of neutrino-produced hadrons is explored using the data collected in the neutrino experiment with bubble chamber SKAT. In Section 2, the experimental procedure is briefly described. The experimental results are presented in Section 3, discussed in Section 4 and summarized in Section 5.

2 Experimental procedure

The experiment was performed with SKAT bubble chamber [1], exposed to a wideband neutrino beam obtained with a 70 GeV primary protons from the Serpukhov accelerator. The chamber was filled with a propan-freon mixture containing 87 vol% propane (C_3H_8) and 13 vol% freon (CF_3Br) with the percentage of nuclei H:C:F:Br = 67.9:26.8:4.0:1.3 %. A 20 kG uniform magnetic field was provided within the operating chamber volume.

Charged current interactions, containing a negative muon with momentum $p_\mu > 0.5$ GeV are selected. Other negatively charged particles are considered to be π^- mesons. Protons with momentum below 0.6-0.65 GeV/c and a fraction of protons with momentum up to 0.85 GeV/c were identified by their stopping in the chamber. More details concerning the experimental procedure, in particular, the event selection criteria and the reconstruction of the neutrino energy E_ν can be found in our previous publications [2, 3, 4, 5]. Each event is given a weight (depending on the charged particle multiplicity) which corrects for the fraction of events excluded due to improperly reconstruction.

For further analysis the events with $3 < E_\nu < 30$ GeV were accepted, provided that the invariant mass of the hadronic system $W > 2$ GeV and the transfer momentum squared $Q^2 > 1$ (GeV/c)². The full sample consists of 2222 events (3167 weighted events). The mean values of the kinematical variables are: $\langle E_\nu \rangle = 10.8$ GeV, $\langle Q^2 \rangle = 3.6$ (GeV/c)², $\langle W \rangle = 3.0$ GeV, $\langle W^2 \rangle = 9.5$ GeV², and, for the energy ν transferred to the hadronic system, $\langle \nu \rangle = 6.5$ GeV.

The whole event sample is subdivided, using several topological and kinematical criteria [4, 5], into three subsamples: the 'cascade' subsample B_S with a sign of intranuclear secondary interactions, the 'quasiproton' (B_p) and 'quasineutron' (B_n) subsamples, the latter two composing the 'quasinucleon' subsample ($B_N \equiv B_p + B_n$) for which no sign of secondary interactions is observed. The corresponding event numbers for B_S , B_p and B_n subsamples are 1190, 477 and 555 (weighted numbers $N_S = 1736$, $N_p = 680$ and $N_n = 751$), respectively. About 40% of subsample B_p is contributed by interactions with free hydrogen. Weighting the 'quasiproton' events with a factor of 0.6, one can compose a 'pure' nuclear sample: $B_A = B_S + B_n + 0.6B_p$ (with an effective atomic weight $\bar{A} = 28$). It could be also shown [4, 5], that a subsample composed as $B_D = B_n + 0.6B_p$ approximately corresponds to the neutrino-deuterium interactions.

3 Experimental results

In present analysis the identified protons are not included. All rest positively (labelled as h^+) and negatively (labelled as π^-) charged hadrons are given the pion mass m_π . The transverse momentum p_T of hadrons is defined with respect to the weak current direction given by the vector difference of the neutrino and muon momenta.

In Fig. 1a the p_T^2 - distributions for h^+ and π^- are plotted for the whole sample of events. Both distributions are fitted to the form $\exp[-b(p_T^2 + m_\pi^2)^{1/2}]$, with parameter $b(h^+) = 5.57 \pm 0.06$ and $b(\pi^-) = 7.48 \pm 0.15$ GeV^{-1} , respectively. The latters are close to those extracted from the neutrino interactions with a heavier composite target (CF_3Br) at the same incident energies [6]. The p_T^2 - distributions for the B_S subsample are less steeper than for the B_N subsample (both shown in Figs. 1b and 1c), owing to an additional transverse momentum acquired by final hadrons in the intranuclear scattering processes. These distributions can be also fitted to the same form resulting in $b_S(h^+) = 5.30 \pm 0.08$ and $b_S(\pi^-) = 7.22 \pm 0.21$ GeV^{-1} for the 'cascade' subsample which are by about 10-15% smaller than those in the 'quasinucleon' subsample, $b_N(h^+) = 6.06 \pm 0.10$ and $b_N(\pi^-) = 7.99 \pm 0.25$ GeV^{-1} . Fig. 2. shows the p_T^2 - distributions for charged hadrons (h^\pm) produced in the current quark and the target fragmentation regions (with Feynman variable $x_F > 0$ and $x_F < 0$, respectively). While at $x_F > 0$ the parameter b is almost the same for subsamples B_N and B_S , $b_N(x_F > 0) = 6.57 \pm 0.12$ $(\text{GeV}/c)^{-1}$ and $b_S(x_F > 0) = 6.43 \pm 0.13$ $(\text{GeV}/c)^{-1}$, at $x_F < 0$ $b_S(x_F < 0) = 5.29 \pm 0.10$ $(\text{GeV}/c)^{-1}$ is by 16% smaller than $b_N(x_F < 0) = 6.13 \pm 0.15$ $(\text{GeV}/c)^{-1}$. The values of $b_N(x_F > 0)$ and $b_N(x_F < 0)$ for the 'quasinucleon' subsample B_N are consistent with those measured in νp [7] and νD [8] interactions at somewhat higher $\langle W^2 \rangle$.

More informative (with respect to the nuclear effects) are the values of $\langle p_T^2 \rangle$ collected in Table 1 for several subsamples and various regions of x_F and W^2 . As it is seen, the nuclear effects influence faintly the $\langle p_T^2 \rangle$ for π^- mesons, as well as for h^+ with $x_F > 0$ both in low ($4 < W^2 < 9$ GeV^2) and high ($9 < W^2 < 25$ GeV^2) regions of W^2 . On the contrary, the $\langle p_T^2 \rangle$ for h^+ with $x_F < 0$ increases by $\Delta(p_T^2) = \langle p_T^2 \rangle_S - \langle p_T^2 \rangle_N = 0.061 \pm 0.013$ $(\text{GeV}/c)^2$ due to the secondary intranuclear interactions. One should emphasize, that this rise is more prominent at $W^2 < 9$ GeV^2 , where $\Delta(p_T^2) = 0.077 \pm 0.016$ $(\text{GeV}/c)^2$, than at $W^2 > 9$ GeV^2 , where $\Delta(p_T^2) = 0.043 \pm 0.021$ $(\text{GeV}/c)^2$. This is in accordance with the recent observations [4, 5, 9] that the effects of the secondary intranuclear interactions are weakening with increasing of W^2 .

Another consequence of the intranuclear interactions is that the region of $x_F > 0$ turns out to be somewhat depleted, while the region of $x_F < 0$ enriched for the subsample B_S relative to the subsample B_N . This can be clearly seen from the data on the mean multiplicities presented in Table 2. The depletion and enrichment effects can be characterized by the ratios $\rho(x_F > 0) = \langle n(x_F > 0) \rangle_S / \langle n(x_F > 0) \rangle_N$ and $\rho(x_F < 0) = \langle n(x_F < 0) \rangle_S / \langle n(x_F < 0) \rangle_N$, respectively. For π^- mesons, the depletion effect is rather weak, $\rho^-(x_F > 0) = 0.92 \pm 0.05$, while the multiplicity gain at $x_F < 0$ reaches $\rho^-(x_F < 0) = 1.66 \pm 0.11$. Slightly larger effects are observed for positively charged hadrons: $\rho^+(x_F > 0) = 0.83 \pm 0.02$ and $\rho^+(x_F < 0) = 1.80 \pm 0.08$. Note, that latter value can be somewhat influenced by the contamination from the non-identified recoil protons emitted during the secondary interaction processes. The lower limit of the mean multiplicity of these protons, evaluated from the identification efficiency for protons with $0.6 < p_p < 0.85$ GeV/c (almost all having $x_F < 0$), turns out to be about 5% of $\langle n_{h^+}(x_F < 0) \rangle_S$. The data of Table 2 also indicate that the depletion and enrichment effects depend on W only slightly.

	$\langle p_T^2 \rangle_N$	$\langle p_T^2 \rangle_S$	$\langle p_T^2 \rangle_D$	$\langle p_T^2 \rangle_A$
$4 < W^2 < 25 \text{ GeV}^2$				
$h^+(x_F > 0)$	0.180 ± 0.006	0.190 ± 0.007	0.182 ± 0.007	0.187 ± 0.005
$\pi^-(x_F > 0)$	0.129 ± 0.009	0.128 ± 0.008	0.131 ± 0.009	0.129 ± 0.006
$h^+(x_F < 0)$	0.207 ± 0.009	0.268 ± 0.009	0.205 ± 0.009	0.252 ± 0.007
$\pi^-(x_F < 0)$	0.126 ± 0.009	0.141 ± 0.008	0.127 ± 0.009	0.137 ± 0.006
$4 < W^2 < 9 \text{ GeV}^2$				
$h^+(x_F > 0)$	0.163 ± 0.007	0.170 ± 0.007	0.161 ± 0.007	0.166 ± 0.005
$\pi^-(x_F > 0)$	0.101 ± 0.009	0.119 ± 0.010	0.104 ± 0.009	0.113 ± 0.007
$h^+(x_F < 0)$	0.189 ± 0.011	0.266 ± 0.011	0.186 ± 0.011	0.245 ± 0.008
$\pi^-(x_F < 0)$	0.106 ± 0.009	0.127 ± 0.009	0.108 ± 0.009	0.122 ± 0.007
$9 < W^2 < 25 \text{ GeV}^2$				
$h^+(x_F > 0)$	0.205 ± 0.012	0.217 ± 0.013	0.214 ± 0.013	0.216 ± 0.009
$\pi^-(x_F > 0)$	0.154 ± 0.015	0.134 ± 0.013	0.156 ± 0.016	0.144 ± 0.010
$h^+(x_F < 0)$	0.228 ± 0.015	0.271 ± 0.014	0.229 ± 0.016	0.259 ± 0.011
$\pi^-(x_F < 0)$	0.149 ± 0.018	0.157 ± 0.019	0.151 ± 0.018	0.155 ± 0.011

Table 1: The mean values of $\langle p_T^2 \rangle$ in $(\text{GeV}/c)^2$ of h^+ and π^- for several subsamples and various regions of x_F and W^2 .

To compare our data with the results of other experiments, as well as to extract quantitative characteristics of the secondary intranuclear interactions, the data on $\langle p_T^2 \rangle$, corresponding to νD and νA interactions, $\langle p_T^2 \rangle_D$ and $\langle p_T^2 \rangle_A$, respectively, are presented in Table 1. The values of $\langle p_T^2 \rangle_D$ and $\langle p_T^2 \rangle_A$ are defined as

$$\langle p_T^2 \rangle_D = \frac{0.6N_p}{N_D} \langle p_T^2 \rangle_p + \frac{N_n}{N_D} \langle p_T^2 \rangle_n, \quad (1)$$

$$\langle p_T^2 \rangle_A = \frac{N_D}{N_A} \langle p_T^2 \rangle_D + \frac{N_S}{N_A} \langle p_T^2 \rangle_S. \quad (2)$$

Here $N_D = N_n + 0.6N_p$, $N_A = N_S + N_D$ and $\langle p_T^2 \rangle_p$ and $\langle p_T^2 \rangle_n$ are the values of $\langle p_T^2 \rangle$ for subsamples B_p and B_n , respectively.

The average multiplicities $\langle n \rangle_A$ and $\langle n \rangle_D$ are defined similarly (see Table 2). The measured values of $\langle p_T^2 \rangle_A - \langle p_T^2 \rangle_D$ and $\langle n \rangle_A - \langle n \rangle_D$ will be compared with theoretical predictions in Section 4.

The dependence of the mean value of $\langle p_T^2 \rangle$ of charged hadrons (combined h^+ and π^-) on the DIS kinematical variables W^2 and ν is presented in Figs. 3 and 4.

	$\langle n \rangle_N$	$\langle n \rangle_S$	$\langle n \rangle_D$	$\langle n \rangle_A$
$4 < W^2 < 25 \text{ GeV}^2$				
$h^+(x_F > 0)$	1.441 ± 0.023	1.198 ± 0.023	1.402 ± 0.023	1.279 ± 0.017
$\pi^-(x_F > 0)$	0.449 ± 0.019	0.412 ± 0.017	0.474 ± 0.019	0.437 ± 0.013
$h^+(x_F < 0)$	0.725 ± 0.023	1.303 ± 0.036	0.677 ± 0.023	1.052 ± 0.024
$\pi^-(x_F < 0)$	0.325 ± 0.017	0.541 ± 0.022	0.339 ± 0.018	0.460 ± 0.015
$4 < W^2 < 9 \text{ GeV}^2$				
$h^+(x_F > 0)$	1.349 ± 0.026	1.106 ± 0.027	1.319 ± 0.026	1.193 ± 0.019
$\pi^-(x_F > 0)$	0.325 ± 0.019	0.309 ± 0.018	0.360 ± 0.021	0.329 ± 0.014
$h^+(x_F < 0)$	0.632 ± 0.027	1.172 ± 0.040	0.589 ± 0.027	0.935 ± 0.027
$\pi^-(x_F < 0)$	0.277 ± 0.019	0.480 ± 0.024	0.295 ± 0.020	0.405 ± 0.016
$9 < W^2 < 25 \text{ GeV}^2$				
$h^+(x_F > 0)$	1.596 ± 0.042	1.349 ± 0.042	1.545 ± 0.042	1.425 ± 0.030
$\pi^-(x_F > 0)$	0.660 ± 0.036	0.579 ± 0.032	0.671 ± 0.036	0.615 ± 0.024
$h^+(x_F < 0)$	0.883 ± 0.043	1.516 ± 0.066	0.829 ± 0.043	1.248 ± 0.044
$\pi^-(x_F < 0)$	0.408 ± 0.032	0.640 ± 0.041	0.417 ± 0.033	0.553 ± 0.028

Table 2: The mean multiplicities of h^+ and π^- for several subsamples and various regions of x_F and W^2 .

It is seen from Fig. 3a, that $\langle p_T^2 \rangle$ for particles with $x_F > 0$ increases with W^2 , as it was observed in earlier investigations with neutrino and muon beams [8, 10, 11, 12, 13, 14]. At the considered range of W^2 , this rise is essentially caused by increase in the available phase space. With increasing of W^2 , the QCD effects are predicted [15] to play more and more significant role in the rise of $\langle p_T^2 \rangle$. The data show (Figs. 3a and 3c), that the nuclear effects practically do not influence $\langle p_T^2 \rangle$ at $x_F > 0$. On the contrary, they cause a significant increase of $\langle p_T^2 \rangle$ at $x_F < 0$ in the region of $W^2 < 15 \text{ GeV}^2$, where the difference $\langle p_T^2 \rangle_A - \langle p_T^2 \rangle_D$ is about $0.04 (\text{GeV}/c)^2$ and practically independent of W^2 .

The dependence of $\langle p_T^2 \rangle$ on ν (see Fig. 4) reveals analogous significant nuclear effects for particles with $x_F < 0$ in the region of $\nu < 9 \text{ GeV}$, where the difference $\langle p_T^2 \rangle_A - \langle p_T^2 \rangle_D$ is around $(0.03-0.05) (\text{GeV}/c)^2$. At ν higher than 9 GeV, the nuclear effects on $\langle p_T^2 \rangle$ are negligible. As for particles with $x_F > 0$, the effects of secondary intranuclear interactions practically do not influence $\langle p_T^2 \rangle$.

The dependence of $\langle p_T^2 \rangle$ for charged hadrons on their kinematical variables is presented in Figs. 5 and 6.

The dependence of $\langle p_T^2 \rangle$ on x_F (Fig. 5a) has a typical 'seagull' form (cf., for example, [6, 11]), both for B_N and B_S subsamples. For the latter, a small part (about 3%) of positively charged hadrons occupies the region of $x_F < -1$, kinematically forbidden for reactions on a

free nucleon (the so called 'cumulative' region), where $\langle p_T^2 \rangle_S$ reaches a rather high value of $\langle p_T^2 \rangle_S \sim 0.6 \text{ (GeV/c)}^2$. About third of these cumulative hadrons are estimated to be non-identified protons with $0.6 < p_p < 0.85 \text{ GeV/c}$ and $\langle p_T^2 \rangle = 0.51 \pm 0.06 \text{ (GeV/c)}^2$. It is seen from Fig. 5b, that the influence of nuclear effects is significant only at $x_F < -0.6$, where the difference $\langle p_T^2 \rangle_A - \langle p_T^2 \rangle_D$ is about $(0.07 \pm 0.03) \text{ (GeV/c)}^2$.

Fig. 6 shows the dependences of $\langle p_T^2 \rangle_N$, $\langle p_T^2 \rangle_S$ and $\langle p_T^2 \rangle_A - \langle p_T^2 \rangle_D$ on the variable $z = E_h/\nu$, the fraction of the current quark energy carried by the hadron. The rise of $\langle p_T^2 \rangle_N$ with z for forward hadrons (Fig. 6c), observed earlier in [10, 11, 13], is mainly caused by the intrinsic transverse momentum of the current quark inside the nucleon [16] (see Section 4 for details). It is seen from Fig. 6b, that the secondary intranuclear interactions induce a significant difference of $\langle p_T^2 \rangle_A - \langle p_T^2 \rangle_D$ almost in the whole range of z . The rise of $\langle p_T^2 \rangle_A - \langle p_T^2 \rangle_D$ at $0 < z < 0.3$ is contributed by particles with $x_F < 0$ (cf. Fig. 6f), while its fall at $z > 0.3$ is caused by the increasing contribution of forward particles for which the difference $\langle p_T^2 \rangle_A - \langle p_T^2 \rangle_D$ is rather small (Fig. 6d).

4 Discussion

The data on $\langle p_T^2 \rangle_N$ of hadrons with $x_F > 0$ in the subsample B_N were checked to be consistent with the conventional picture of the quark string fragmentation (see e.g. [16] for review). According to the latter, the z -dependence of $\langle p_T^2 \rangle_N$ for leading hadrons (containing the current quark) can be parameterized as [17]:

$$\langle p_T^2 \rangle_N = \langle p_T^2 \rangle_{Frag} + z^2 \langle k_T^2 \rangle + \langle p_T^2 \rangle_{QCD}, \quad (3)$$

where $\langle p_T^2 \rangle_{Frag}$ is the contribution from the fragmentation process, k_T is the primordial transverse momentum of the current quark inside the nucleon, while $\langle p_T^2 \rangle_{QCD}$ is the contribution of QCD effects (involving hard gluon emission and $q\bar{q}$ production). At W^2 available in this experiment ($W^2 < 25 \text{ GeV}^2$), the latter term can be approximately parameterized as [18]

$$\langle p_T^2 \rangle_{QCD} = a(W^2 - W_0^2), \quad (4)$$

with $a = 3.5 \cdot 10^{-3} \text{ (GeV/c)}^2$ and $W_0^2 = 2 \text{ GeV}^2$.

Fig. 7 shows the z^2 -dependence for $\langle p_T^2 \rangle$ of positively charged hadrons in the current fragmentation region for two intervals of W^2 , $W^2 < 9 \text{ GeV}^2$ and $W^2 > 9 \text{ GeV}^2$ (containing approximately equal statistics). The data for fast hadrons (with $z^2 > 0.16$), containing with a high probability the current quark, are fitted to dependence (3). The QCD term in (3) was fixed according to (4). At $z^2 > 0.16$ the mean value of $\langle W^2 \rangle$ in present experiment is practically independent of z^2 : $\langle W^2 \rangle \approx 6 \text{ GeV}^2$ leading to $\langle p_T^2 \rangle_{QCD} = 0.014 \text{ (GeV/c)}^2$ for the region $W^2 < 9 \text{ GeV}^2$, and $\langle W^2 \rangle \approx 14 \text{ GeV}^2$ leading to $\langle p_T^2 \rangle_{QCD} = 0.042 \text{ (GeV/c)}^2$ for the region $W^2 > 9 \text{ GeV}^2$. The fit results are plotted in Figs. 7a and 7b. The fitted values of $\langle p_T^2 \rangle_{Frag}$ and $\langle k_T^2 \rangle$ turn out to be independent of W^2 within statistical uncertainties: $\langle p_T^2 \rangle_{Frag} = 0.17 \pm 0.03 \text{ (GeV/c)}^2$, $\langle k_T^2 \rangle = 0.23 \pm 0.10 \text{ (GeV/c)}^2$ at $W^2 < 9 \text{ GeV}^2$, and $\langle p_T^2 \rangle_{Frag} = 0.22 \pm 0.07 \text{ (GeV/c)}^2$, $\langle k_T^2 \rangle = 0.30 \pm 0.19 \text{ (GeV/c)}^2$ at $W^2 > 9 \text{ GeV}^2$.

The quoted values of $\langle k_T^2 \rangle$ are consistent with those extracted from the data on νp [19] and μp [20, 21] deep inelastic scattering at higher W^2 ($16 < W^2 < 400 \text{ GeV}^2$). The values of $\langle p_T^2 \rangle_{Frag}$ are also consistent with that estimated in [19], however somewhat underestimate the value of $\langle p_T^2 \rangle_{Frag} = 0.274 \pm 0.059$ extracted from e^+e^- annihilation at the LEP energies

[22].

In Fig. 7c the difference $\langle p_T^2 \rangle_A - \langle p_T^2 \rangle_D$ versus z^2 is plotted. The data at low W^2 , $W^2 < 9 \text{ GeV}^2$, indicate, that the additional transverse momentum, acquired by forward hadrons (with $x_F > 0$) due to the intranuclear interactions, slightly increases with z , while at larger $W^2 > 9 \text{ GeV}^2$ no significant nuclear effects are observed.

Below an attempt is undertaken to describe the obtained experimental data on differences $\langle n \rangle_A - \langle n \rangle_D$ and $\langle p_T^2 \rangle_A - \langle p_T^2 \rangle_D$, which characterize the strength of nuclear effects, with the help of a simple model incorporating the secondary intranuclear interactions of produced pions. We assume that the formation length l_π of pions is determined [23] in the framework of the Lund fragmentation model [24]:

$$l_\pi = \nu z \left[\frac{\ln(1/z^2) - 1 + z^2}{1 - z^2} \right] / k, \quad (5)$$

where $k \approx 1 \text{ GeV/fm}$ is the quark string tension. The expression (5) has a maximum at $z \approx 0.3$ and behaves as $l_\pi \approx 2\nu z \ln(0.61/z)/k$ at $z < 0.2$ and approximately (with an accuracy better than 20%) as $l_\pi \approx \nu(1 - z)/k$ at $z > 0.5$. The latter behaviour (predicted also in [25]) was found to be consistent with recent experimental data [4, 5, 26]. We assume, that a pion can interact in the nucleus, starting from the distance l_π from the νN scattering point. The hadrons (predominantly pions) produced in νN interactions at $x_F > 0$ carry relatively large momenta, the mean values $\bar{p}_\pi(x_F > 0)$ of which are presented in the Appendix (Table A1) for two regions of W^2 , $W^2 < 9 \text{ GeV}^2$ and $W^2 > 9 \text{ GeV}^2$. We assume, that these pions undergo intranuclear inelastic interactions with pion-nucleon cross section $\sigma_{\pi N}^{in}$ (averaged over protons and neutrons of the target nuclei). The estimated cross sections are around $\sigma_{\pi N}^{in} \approx 21\text{--}24 \text{ mb}$ [27, 28], depending on $\bar{p}_\pi(x_F > 0)$. With these cross sections, the probabilities w_{in} of secondary interactions averaged over l_π and nuclei of the propane-freon mixture are calculated (see [4, 5] for details). The values of w_{in} are given in Table A1. The average multiplicities $\bar{n}(\pi \rightarrow \pi')$ of secondary π^+ and π^- mesons in reactions $\pi N \rightarrow \pi X$ at given average momenta $\bar{p}_\pi(x_F > 0)$ are estimated using the partial πN cross sections [27] (see Table A1). Further one may assume, that a fraction β of secondary pions occupies the region of $x_F < 0$, while the remaining fraction $(1 - \beta)$ stays in the region of $x_F > 0$. The parameter β (a free parameter of the model) is expected to differ for like-sign pions, i.e. for $\pi^+(\pi^-)$ mesons in $\pi^+(\pi^-)$ -induced reactions and for unlike-sign pions, i.e. for $\pi^-(\pi^+)$ mesons in $\pi^+(\pi^-)$ -induced reactions. For unlike-sign pions $\beta_u \sim 1$ is expected, because they acquire a small fraction of the parent pion energy and hence occupy predominantly the region of $x_F < 0$. A value of $\beta_u = 0.9 \pm 0.1$ is chosen as a result. The parameter β_l for like-sign pions has to be smaller than for unlike-sign pions, $\beta_l < \beta_u$, due to the leading hadron effect. A value of $\beta_l = 0.67 \pm 0.10$ is chosen to fit the data on measured quantity $\langle n_{\pi^\pm}(x_F > 0) \rangle_A - \langle n_{\pi^\pm}(x_F > 0) \rangle_D$ characterizing the attenuation of the π^\pm yield in the forward hemisphere of νA interactions as compared to that in νD interactions.

The intranuclear interactions of produced π^0 mesons should be taken into account also. It is expected that all relevant quantities concerning π^0 are in between those for π^+ and π^- (see [29] and references therein). For simplicity they are taken as averages of those for π^+ and π^- mesons, with a maximal uncertainty. For example, the parameter β_0 for π^0 -induced reactions, is taken to be $\beta_0 = 0.5(\beta_l + \beta_u)$ with uncertainty $\Delta\beta_0 = \pm 0.5(\beta_l - \beta_u)$.

With the above quantities, characterizing the secondary inelastic interactions, one can write down expressions (given by eqs. A1 and A2 in the Appendix) for the predicted multiplicity differences $\langle n_\pi \rangle_A - \langle n_\pi \rangle_D$ of pions produced in νA and νD interactions at $x_F > 0$ and $x_F < 0$. A comparison with the experimental data is given in Table 3.

range of $W^2(\text{GeV}^2)$	particle type	$\langle n \rangle_A - \langle n \rangle_D$	
		measured	calculated
$4 < W^2 < 9$	$h^+(x_F > 0)$	-0.123 ± 0.019	-0.136 ± 0.045
	$\pi^-(x_F > 0)$	-0.037 ± 0.015	-0.008 ± 0.032
	$h^+(x_F < 0)$	0.375 ± 0.025	0.407 ± 0.084
	$\pi^+(x_F < 0)$	—	0.318 ± 0.082
	$\pi^-(x_F < 0)$	0.121 ± 0.017	0.241 ± 0.069
$9 < W^2 < 25$	$h^+(x_F > 0)$	-0.119 ± 0.036	-0.059 ± 0.041
	$\pi^-(x_F > 0)$	-0.056 ± 0.029	-0.006 ± 0.039
	$h^+(x_F < 0)$	0.418 ± 0.048	0.284 ± 0.051
	$\pi^+(x_F < 0)$	—	0.234 ± 0.050
	$\pi^-(x_F < 0)$	0.136 ± 0.032	0.186 ± 0.044

Table 3: The measured and predicted differences $\langle n \rangle_A - \langle n \rangle_D$ at $x_F > 0$ and $x_F < 0$.

A reasonable consistency with the data at $x_F > 0$ is observed. Particularly, the model predicts a stronger depletion for the yield of h^+ than for π^- in the forward hemisphere in agreement with the data. The data description at $x_F < 0$ is worse. The model overestimates the enhancement of the π^- yield at $W^2 < 9 \text{ GeV}^2$ by factor two, but is in agreement with the data at $W^2 > 9 \text{ GeV}^2$ within experimental uncertainties. On the other hand, the predicted values of $\langle n_{\pi^+}(x_F < 0) \rangle_A - \langle n_{\pi^+}(x_F < 0) \rangle_D$ are smaller than the measured values for h^+ , especially at $W^2 > 9 \text{ GeV}^2$.

As it was already mentioned, the positively charged hadrons with $x_F < 0$ in the subsample B_S (and B_A) include non-identified protons with $p_p > 0.6 \text{ GeV}/c$. The latter originate from secondary interactions of produced pions, both from inelastic interactions (of pions with $x_F > 0$) and elastic πp scattering of pions with $x_F > 0$ and $x_F < 0$ (average momenta are given in Table A1). The probability of the intranuclear scattering $\pi p \rightarrow \pi p$ convoluted with the probability of non-identification of the recoil proton is estimated using the differential cross section of $\pi^\pm p \rightarrow \pi^\pm p$ [28]. The corresponding expressions for the mean multiplicity $\langle n_p^{nid} \rangle_{el}$ of non-identified recoil protons are given in the Appendix (eqs. A3 and A4). The calculated value of $\langle n_p^{nid} \rangle_{el}$, taking into account the contribution from $\pi^0 p \rightarrow \pi^0 p$ also, turns out to be 0.042 ± 0.011 at $W^2 < 9 \text{ GeV}^2$ and 0.023 ± 0.006 at $W^2 > 9 \text{ GeV}^2$.

The probability of inelastic reactions $\pi N \rightarrow pX$ convoluted with the probability of non-identification of the recoil proton can be estimated using the differential cross section $d\sigma_{in}/dt$, where t is the squared four-momentum transferred to proton. As there are no data available for cross sections of inclusive reactions $\pi N \rightarrow pX$ at the relevant momentum range of the projectile pion, the data [28] on exclusive channels were used. The data can be parametrized as $d\sigma_{in}^p/dt = a_1 \exp(b'_p t) + a_2 \exp(b''_p t)$ with $b'_p = 5 \pm 2 (\text{GeV}/c)^{-2}$ and $b''_p = 1.5 \pm 0.5 (\text{GeV}/c)^{-2}$. The coefficients a_1 and a_2 are extracted from the compilations [27, 28]. The corresponding expression for $\langle n_p^{nid} \rangle_{inel}$ is given in the Appendix (eq. A5). The calculated value of $\langle n_p^{nid} \rangle_{inel}$, taking into account the contribution from $\pi^0 N \rightarrow pX$ also, turns out to be 0.047 ± 0.020 at $W^2 < 9 \text{ GeV}^2$ and 0.027 ± 0.010 at $W^2 > 9 \text{ GeV}^2$. Using the summary multiplicity $\langle n_p^{nid} \rangle = \langle n_p^{nid} \rangle_{el} + \langle n_p^{nid} \rangle_{inel}$, the overwhelming fraction of which refers to the region of $x_F < 0$, one obtains predictions for

$$\begin{aligned}
& \langle n_{h^+}(x_F < 0) \rangle_A - \langle n_{h^+}(x_F < 0) \rangle_D = \\
& \langle n_{\pi^+}(x_F < 0) \rangle_A + \langle n_p^{nid} \rangle - \langle n_{\pi^+}(x_F < 0) \rangle_D,
\end{aligned} \tag{6}$$

assuming $\langle n_{h^+}(x_F < 0) \rangle_D \approx \langle n_{\pi^+}(x_F < 0) \rangle_D$ for νD interactions. The latter correction, as one may observe, slightly improves the agreement with the data on $\langle n_{h^+}(x_F < 0) \rangle_A - \langle n_{h^+}(x_F < 0) \rangle_D$. A significant discrepancy, however, remains for the data at $W^2 > 9 \text{ GeV}^2$. Nevertheless, the model reproduces the nuclear depletion and enhancement effects for the yield of h^+ and π^- qualitatively and, in particular, predicts, in accordance with the experimental observation, these effects to be more significant for h^+ than for π^- .

A further application of the model concerns the description of the data on $\langle p_T^2 \rangle$ presented in Table 1, namely, on the difference $\langle p_T^2 \rangle_A - \langle p_T^2 \rangle_D$, being caused by secondary intranuclear interactions of produced hadrons, both elastic and inelastic.

The elastic πN cross sections $\sigma_{el}(|t| > t_{min})$ are extracted from the data [28] on differential cross sections integrated over the region of $|t| > t_{min} = 0.05 \text{ (GeV/c)}^2$. The latter restriction is introduced in order to take into account the Pauli blocking effect, i.e. the suppression of the intranuclear scattering with small four-momenta transferred to the bound nucleon. The probability w_{el} of the elastic scattering (provided that the pion did not undergo any inelastic interaction) is calculated at average momenta \bar{p}_π of π^+ and π^- mesons with $x_F > 0$ and $x_F < 0$ (see Table A1). The average $\langle p_T^2 \rangle_{el}^{\pi N}$ acquired by the elastically scattered pion (with respect to the 'projectile' one) varies from 0.09 to 0.26 $(\text{GeV/c})^2$, depending on \bar{p}_π and the pion sign. The corresponding values with respect to the weak current direction, $\langle p_T^2 \rangle_{el}$, can be obtained as

$$\langle p_T^2 \rangle_{el}^\pi = \langle p_T^2 \rangle_{el}^{\pi N} \left(1 - \frac{3}{2} \langle \sin^2 \vartheta_\pi \rangle\right) + p_{sc}^2 \langle \sin^2 \vartheta_\pi \rangle, \quad (7)$$

where p_{sc} is the momentum of the scattered pion, while ϑ_π is the polar angle of the 'projectile' pion with respect to the weak current axis. The estimated values of $\langle p_T^2 \rangle_{el}^\pi$ are given in Table A1.

As for inelastic interactions of pions with $x_F > 0$, there are no data on inclusive characteristics of reactions $\pi^+ N \rightarrow \pi^\pm X$ and $\pi^- N \rightarrow \pi^\mp X$ at the relevant incident momenta. Therefore, $\langle p_T^2(\pi \rightarrow \pi') \rangle_{in}$ is considered as a free parameter of the model (for the each incident momentum and the reaction type). The general expectation is that it increases with the incident momentum and is larger for like-sign pions than for unlike-sign ones [30]. In addition, the final pions occupying the region of $x_F < 0$ are expected to have on an average larger $\langle p_T^2(\pi \rightarrow \pi') \rangle_{in}^b$ than those with $x_F > 0$, $\langle p_T^2(\pi \rightarrow \pi') \rangle_{in}^f$, due to the Lorentz transformation from the πN c.m.s. to the c.m.s. of the hadronic system. The chosen values of $\langle p_T^2(\pi \rightarrow \pi') \rangle_{in}^f$ and $\langle p_T^2(\pi \rightarrow \pi') \rangle_{in}^b$ with respect to the weak current axis are given in the Appendix (Table A2). One should note, that the maximal value of $\langle p_T^2(\pi^+ \rightarrow \pi^+) \rangle_{in}^b = 0.3 \text{ (GeV/c)}^2$ refers to the like-sign pion with $x_F < 0$ in reaction $\pi^+ N \rightarrow \pi^+(x_F < 0)X$, while the minimal value of $\langle p_T^2(\pi^- \rightarrow \pi^+) \rangle_{in}^f = 0.1 \text{ (GeV/c)}^2$ refers to the unlike-sign pion with $x_F > 0$ in reaction $\pi^- N \rightarrow \pi^+(x_F > 0)X$.

Using all above defined quantities, and taking into account the contribution from π^0 - induced reactions $\pi^0 N \rightarrow \pi^\pm X$ also, predictions for $\langle p_T^2 \rangle_A$ can be obtained (see eqs. A6 and A7 in the Appendix). The predicted and measured values for the difference $\langle p_T^2 \rangle_A - \langle p_T^2 \rangle_D$ are presented in Table 4. The model reproduces rather small values of this difference at $x_F > 0$, as well as the data for π^- mesons with $x_F < 0$. A reasonable agreement with the data on $\langle p_T^2(x_F < 0) \rangle_A^+ - \langle p_T^2(x_F < 0) \rangle_D^+$ is obtained when taking into account the contribution from non-identified protons (see eq. A7 of the Appendix). The quoted errors in Table 4 for predicted values include only the uncertainty in parameters β_u , β_l and β_0 and in the contribution from π^0 - induced reactions, but do not that in the chosen values of

$\langle p_T^2 \rangle_{in}$ (quoted in Table A2 of the Appendix).

range of $W^2(\text{GeV}^2)$	particle type	$\langle p_T^2 \rangle_A - \langle p_T^2 \rangle_D (\text{GeV}/c)^2$	
		measured	calculated
$4 < W^2 < 9$	$h^+(x_F > 0)$	0.005 ± 0.006	0.003 ± 0.008
	$\pi^-(x_F > 0)$	0.009 ± 0.008	0.001 ± 0.011
	$h^+(x_F < 0)$	0.059 ± 0.009	0.032 ± 0.019
	$\pi^+(x_F < 0)$	—	0.020 ± 0.020
	$\pi^-(x_F < 0)$	0.014 ± 0.008	0.036 ± 0.024
$9 < W^2 < 25$	$h^+(x_F > 0)$	0.002 ± 0.011	0.000 ± 0.012
	$\pi^-(x_F > 0)$	-0.012 ± 0.013	-0.002 ± 0.015
	$h^+(x_F < 0)$	0.030 ± 0.013	0.010 ± 0.016
	$\pi^+(x_F < 0)$	—	0.006 ± 0.016
	$\pi^-(x_F < 0)$	0.004 ± 0.008	0.016 ± 0.019

Table 4: The measured and predicted differences $\langle p_T^2 \rangle_A - \langle p_T^2 \rangle_D$ at $x_F > 0$ and $x_F < 0$.

More definite predictions for $\langle p_T^2 \rangle_A - \langle p_T^2 \rangle_D$ can be obtained for leading hadrons (the experimental data for which are plotted in Fig. 7c). For the subsample B_A , these hadrons can be subdivided into two fractions. The first one consists of hadrons which escape the nucleus without any interaction (with a probability w_e) and for which the value of $\langle p_T^2 \rangle_D$ is preserved. The second fraction consists of hadrons which have undergone only an elastic scattering (with a probability w_{el}^f) with a moderate momentum transfer $|t| < t_{max}$ (in order to be survived as a large $-z$ particle) and which acquire on an average $\langle p_T^2 \rangle_{el}$ with respect to the weak current axis. The values of $|t|$ in the range of $|t| < t_{max}$ correspond to the scattering angle $\vartheta_\pi^* < 90^\circ$ in the πN c.m.s. at which the pion keeps on an average more than 90% of its energy. The value of $\langle p_T^2 \rangle_{el}$ is extracted using the data [28] on $d\sigma_{el}^{\pi N}/dt$ in the range of $t_{min} < |t| < t_{max}$ and the relation (7) to transform it with respect to the weak current axis.

The relative weights of these two fractions of the leading hadrons are $w_e/(w_e + w_{el}^f)$ and $w_{el}^f/(w_e + w_{el}^f)$, respectively. As a result,

$$\langle p_T^2 \rangle_A - \langle p_T^2 \rangle_D = \frac{w_{el}^f}{w_e + w_{el}^f} (\langle p_T^2 \rangle_{el} - \langle p_T^2 \rangle_D). \quad (8)$$

The predicted values of (8) are compared with the data plotted in Fig. 7a for positively charged leading hadrons with $0.16 < z^2 < 0.3$ and $z^2 > 0.3$ (at $W^2 < 9 \text{ GeV}^2$). In these intervals, the particles are characterized by the following measured and calculated quantities: $\bar{p}_{h^+} = 2.0$ and $2.9 \text{ GeV}/c$, $\langle p_T^2 \rangle_D = 0.227 \pm 0.015$ and $0.297 \pm 0.024 (\text{GeV}/c)^2$; $\bar{l}_h = 1.9$ and 1.1 fm , $\sigma_{el}^f(t_{min} < |t| < t_{max}) = 5.3$ and 4.2 mb , $\sigma'_{tot} = \sigma_{in}^{\pi N} + \sigma'_{el}(|t| > t_{min}) = 28.5$ and 27.7 mb , $w_{el}^f = 0.030$ and 0.029 , $w_e = 0.754$ and 0.668 , $\langle p_T^2 \rangle_{el} = 0.411$ and $0.489 (\text{GeV}/c)^2$, respectively. With these values, one obtains for the difference $\langle p_T^2 \rangle_A - \langle p_T^2 \rangle_D = 0.007 \pm 0.001$ and $0.008 \pm 0.001 (\text{GeV}/c)^2$ at $0.16 < z^2 < 0.3$ and $z^2 > 0.3$, respectively.

The corresponding quantities for h^+ with $z^2 > 0.2$ (at $W^2 > 9 \text{ GeV}^2$) are: $\bar{p}_{h^+} = 6.1 \text{ GeV}/c$, $\langle p_T^2 \rangle_D = 0.401 \pm 0.042 (\text{GeV}/c)^2$; $\bar{l}_h = 3.3 \text{ fm}$, $\sigma_{el}^f(t_{min} < |t| < t_{max}) = 3.5 \text{ mb}$, $\sigma'_{tot} = 20.8 \text{ mb}$, $w_{el}^f = 0.017$, $w_e = 0.832$ and $\langle p_T^2 \rangle_{el} = 0.68 (\text{GeV}/c)^2$, leading to $\langle p_T^2 \rangle_A - \langle p_T^2 \rangle_D = 0.006 \pm 0.001 (\text{GeV}/c)^2$. The predicted values of $\langle p_T^2 \rangle_A - \langle p_T^2 \rangle_D$ for leading particles

are rather small in agreement with the data and do not contradict the trend of the latters with variation of z^2 and W^2 , as it can be seen from Fig. 7c.

Finally, one needs to note, that although the applied model reproduces the majority of the experimental data (presented in Tables 3 and 4 and Fig. 7c), it is rather crude and uses several simplified assumptions which should be summarized: i) the calculations concerning the secondary intranuclear interactions are performed for fixed average momenta of π^+ and π^- mesons, $\bar{p}_{\pi^\pm}(x_F > 0)$ and $\bar{p}_{\pi^\pm}(x_F < 0)$, instead of more extensive calculations averaged over the momentum spectra; ii) the second-order effects of two or more intranuclear collisions of a pion are neglected; iii) the model does not incorporate the production of hadronic resonances, in particular, ρ mesons (composing about 10% of charged pions [31, 32]), with a proper space-time structure of their formation, intranuclear interactions and decay.

5 Summary

New experimental data concerning the influence of the nuclear medium on the transverse momentum of neutrino-produced hadrons are presented.

The p_T^2 - distribution of hadrons (both positively and negatively charged) is less steeper in 'cascading' (and 'nuclear') than in 'quasinucleon' (and 'quasideuteron') interactions. The influence of the nuclear medium on the dependence of $\langle p_T^2 \rangle$ on kinematical variables of the DIS and of final hadrons is studied. The nuclear effects, leading to an enhancement of $\langle p_T^2 \rangle$, are more prominent for the following ranges of variables:

- for $x_F < 0$ at $W^2 < 15 \text{ GeV}^2$ or $\nu < 9 \text{ GeV}$, while no significant enhancement of $\langle p_T^2 \rangle$ is observed at higher W^2 or ν ;
- for $x_F < -0.6$, while at $x_F > -0.6$ the manifestation of nuclear effects is faint;
- practically for the whole range of z .

The observed z^2 - dependence of $\langle p_T^2 \rangle_N$ for fast hadrons in the 'quasinucleon' subsample follows the conventional picture of the quark string fragmentation. The extracted parameters governing the transverse momentum of produced hadrons, $\langle p_T^2 \rangle_{Frag} = 0.19 \pm 0.03 (\text{GeV}/c)^2$ and $\langle k_T^2 \rangle = 0.24 \pm 0.09 (\text{GeV}/c)^2$ (estimated for the whole range of $4 < W^2 < 25 \text{ GeV}^2$), are compatible with values obtained at higher energies.

The experimental data on nuclear effects are compared with predictions of a simple model incorporating the secondary intranuclear interactions of produced hadrons. The model predicts a depletion of the particle yield at $x_F > 0$ and an enhancement of that at $x_F < 0$ (more pronounced for positively charged hadrons for both regions of $x_F > 0$ and $x_F < 0$) in agreement with the data. The quantitative description of the most part of the data on the hadron yields is also acceptable. The model describes also the data on the difference $\langle p_T^2 \rangle_A - \langle p_T^2 \rangle_D$ both for h^+ and π^- with $x_F > 0$ and $x_F < 0$, as well as for the leading particles with $z > 0.4$. It has been shown, that the model predictions for differences $\langle n_{h^+}(x_F < 0) \rangle_A - \langle n_{h^+}(x_F < 0) \rangle_D$ and $\langle p_T^2(x_F < 0) \rangle_A^+ - \langle p_T^2(x_F < 0) \rangle_D^+$ for positively charged hadrons with $x_F < 0$ turn out to be in better agreement with the data, when taking into account the contribution from non-identified protons.

Acknowledgement: The activity of one of the authors (Zh.K.) is supported by Cooperation Agreement between DESY and YerPhI signed on December 6, 2002.

Appendix

The mean multiplicity of π^+ mesons with $x_F > 0$ and $x_F < 0$ in νA interactions can be approximately expressed, taking into account the intranuclear inelastic interactions of produced pions, as:

$$\begin{aligned} < n_{\pi^+}(x_F > 0) >_A = (1 - w_{in}^+) < n_{\pi^+}(x_F > 0) >_D \\ &+ \sum_{i=1}^3 w_{in}^i < n_{\pi^i}(x_F > 0) >_D (1 - \beta_i) \bar{n}(\pi^i \rightarrow \pi^+) \end{aligned} \quad (A1)$$

$$\begin{aligned} < n_{\pi^+}(x_F < 0) >_A = < n_{\pi^+}(x_F < 0) >_D \\ &+ \sum_{i=1}^3 w_{in}^i < n_{\pi^i}(x_F > 0) >_D \beta_i \bar{n}(\pi^i \rightarrow \pi^+). \end{aligned} \quad (A2)$$

where the index i refers to the pion species, π^+, π^-, π^0 . The first term in (A1) corresponds to π^+ mesons produced in νN (or νD) interactions with $x_F > 0$ and not suffered inelastic interactions. The last three terms correspond to π^+ mesons produced in secondary inelastic interactions $\pi^+ N \rightarrow \pi^+ X$, $\pi^- N \rightarrow \pi^+ X$ and $\pi^0 N \rightarrow \pi^+ X$, having mean multiplicities $\bar{n}(\pi^+ \rightarrow \pi^+)$, $\bar{n}(\pi^- \rightarrow \pi^+)$ and $\bar{n}(\pi^0 \rightarrow \pi^+)$, and occupying the region of $x_F > 0$ with probabilities $(1 - \beta_l)$, $(1 - \beta_u)$ and $(1 - \beta_0)$, respectively. The first term in (A2) corresponds to π^+ mesons with $x_F < 0$ in νD interactions. The secondary inelastic interactions of these mesons play a negligible role, because their average momentum is small (see Table A1). We neglect also the charge-exchange reactions $\pi^+ n \rightarrow \pi^0 p$ and $\pi^0 p \rightarrow \pi^+ n$, the summary contribution of which to the mean multiplicity of final π^+ mesons is expected to be largely cancelled. The last three terms in (A2) correspond to π^+ mesons produced in secondary inelastic interactions (mentioned above) and occupying the region of $x_F < 0$ with probabilities β_l , β_u and β_0 for π^+ , π^- and π^0 - induced reactions, respectively. Similar expressions can be written down for the mean multiplicity of π^- mesons, $< n_{\pi^-}(x_F > 0) >_A$ and $< n_{\pi^-}(x_F < 0) >_A$. The values of w_{in}^+ , w_{in}^- , w_{in}^0 , $\bar{n}(\pi^+ \rightarrow \pi^\pm)$, $\bar{n}(\pi^- \rightarrow \pi^\pm)$ and $\bar{n}(\pi^0 \rightarrow \pi^\pm)$ are given in Table A1, while β_l , β_u , and β_0 are defined in Section 4.

Contributions to the multiplicity of positively charged hadrons, $< n_{h^+}(x_F < 0) >_A$, comes from $< n_{\pi^+}(x_F < 0) >_A$ and non-identified recoil protons with $p_p > 0.6$ GeV/c, the overwhelming part of which occupies the region of $x_F < 0$. The mean multiplicity of these protons can be expressed as follows:

i) The contribution from πp elastic scattering of π^+ , π^- and π^0 mesons with $x_F > 0$, which scatter with probabilities $w_{el}^+(f)$, $w_{el}^-(f)$ and $w_{el}^0(f)$ (see Table A1), respectively:

$$< n_p^{nid} >_{el}' = \sum_{i=1}^3 w_{el}^i(f) < n_{\pi^i}(x_F > 0) >_D < n_p^{nid} >_{\pi_f^i p}^{el}, \quad (A3)$$

where $< n_p^{nid} >_{\pi_f^+ p}^{el} = 0.4$, $< n_p^{nid} >_{\pi_f^- p}^{el} = 0.27$, $< n_p^{nid} >_{\pi_f^0 p}^{el} = 0.34$ at $W^2 < 9$ GeV², resulting in $< n_p^{nid} >_{el}' = 0.038$, and $< n_p^{nid} >_{\pi_f^+ p}^{el} = 0.13$, $< n_p^{nid} >_{\pi_f^- p}^{el} = 0.19$, $< n_p^{nid} >_{\pi_f^0 p}^{el} = 0.16$, resulting in $< n_p^{nid} >_{el}' = 0.004$ at $W^2 > 9$ GeV².

ii) The contribution from πp elastic scattering of π^+ , π^- , and π^0 mesons with $x_F < 0$, which scatter with probabilities $w_{el}^+(b)$, $w_{el}^-(b)$ and $w_{el}^0(b)$, respectively (see Table A1):

$$\langle n_p^{nid} \rangle_{el}'' = \sum_{i=1}^3 w_{el}^i(b) \langle n_{\pi^i}(x_F < 0) \rangle_D \langle n_p^{nid} \rangle_{\pi_b^i p}^{el}, \quad (A4)$$

where $\langle n_p^{nid} \rangle_{\pi_b^+ p}^{el} = 0.05$, $\langle n_p^{nid} \rangle_{\pi_b^- p}^{el} = 0.09$, $\langle n_p^{nid} \rangle_{\pi_b^0 p}^{el} = 0.07$ at $W^2 < 9 \text{ GeV}^2$, resulting in $\langle n_p^{nid} \rangle_{el}'' = 0.004$, and $\langle n_p^{nid} \rangle_{\pi_b^+ p}^{el} = 0.22$, $\langle n_p^{nid} \rangle_{\pi_b^- p}^{el} = 0.27$, $\langle n_p^{nid} \rangle_{\pi_b^0 p}^{el} = 0.24$, resulting in $\langle n_p^{nid} \rangle_{el}'' = 0.018$ at $W^2 > 9 \text{ GeV}^2$.

iii) The contribution from πN inelastic interactions of π^+ , π^- and π^0 mesons with $x_F > 0$, which interact with probabilities w_{in}^+ , w_{in}^- and w_{in}^0 , respectively (see Table A1):

$$\langle n_p^{nid} \rangle_{inel} = \sum_{i=1}^3 w_{in}^i \langle n_{\pi^i}(x_F < 0) \rangle_D \langle n_p^{nid} \rangle_{\pi^i p}^{in}, \quad (A5)$$

where $\langle n_p^{nid} \rangle_{\pi^+ N}^{in} \approx \langle n_p^{nid} \rangle_{\pi^- N}^{in} \approx \langle n_p^{nid} \rangle_{\pi^0 N}^{in} \approx 0.16$ at $W^2 < 9 \text{ GeV}^2$, resulting in $\langle n_p^{nid} \rangle_{inel} = 0.047$, and $\langle n_p^{nid} \rangle_{\pi^+ N}^{in} \approx \langle n_p^{nid} \rangle_{\pi^- N}^{in} \approx \langle n_p^{nid} \rangle_{\pi^0 N}^{in} \approx 0.17$, resulting in $\langle n_p^{nid} \rangle_{inel} = 0.027$ at $W^2 > 9 \text{ GeV}^2$.

The summary multiplicity of non-identified protons is $\langle n_p^{nid} \rangle = \langle n_p^{nid} \rangle_{el}' + \langle n_p^{nid} \rangle_{el}'' + \langle n_p^{nid} \rangle_{inel} = 0.089$ at $W^2 < 9 \text{ GeV}^2$ and 0.049 at $W^2 > 9 \text{ GeV}^2$. These values have to be added to (A2) to obtain $\langle n_{h^+}(x_F < 0) \rangle_A = \langle n_{\pi^+}(x_F < 0) \rangle_A + \langle n_p^{nid} \rangle$.

Different fractions of π^+ mesons in (A1)-(A2) or of positively charged hadrons in (A1)-(A5) carry different values of $\langle p_T^2 \rangle$. Hence, the mean value of $\langle p_T^2 \rangle_A$ has to be expressed as a superposition of different terms. For example, the expressions for $\langle p_T^2(x_F > 0) \rangle_A^+$ and $\langle p_T^2(x_F < 0) \rangle_A^+$ have the following form:

$$\langle p_T^2(x_F > 0) \rangle_A^+ = \sum_{i=1}^5 \alpha_i^f \langle p_T^2 \rangle_i^f \quad (A6)$$

$$\langle p_T^2(x_F < 0) \rangle_A^+ = \sum_{i=1}^{14} \alpha_i^b \langle p_T^2 \rangle_i^b \quad (A7)$$

where α_i^f (α_i^b) is the normalized part of the i -th fraction of h^+ occupying the region of $x_F > 0$ ($x_F < 0$).

The first term in (A6) corresponds to 'primary' π^+ mesons with $x_F > 0$ produced in νN -interactions, which do not suffer any secondary interaction within the nucleus and hence keep the value of $\langle p_T^2(x_F > 0) \rangle_D^+$. The second term corresponds to π^+ mesons with $x_F > 0$, which have suffered an elastic scattering (but not any inelastic interaction) and acquired $\langle p_T^2(x_F > 0) \rangle_{el}^+$ (given in Table A1). The last three terms correspond to π^+ mesons which are produced in secondary inelastic interactions of 'primary' π^+ , π^- and π^0 and have occupied the region of $x_F > 0$, acquiring $\langle p_T^2(\pi^+ \rightarrow \pi^+) \rangle_{in}^f$, $\langle p_T^2(\pi^- \rightarrow \pi^+) \rangle_{in}^f$ and $\langle p_T^2(\pi^0 \rightarrow \pi^+) \rangle_{in}^f$, respectively. The latter are free parameters of the model and are presented in Table A2.

The first term in (A7) corresponds to 'primary' π^+ mesons with $x_F < 0$, which do not suffer

any interaction and hence keep the value of $\langle p_T^2(x_F < 0) \rangle_D^+$. The second term corresponds to 'primary' π^+ mesons with $x_F < 0$, which have suffered an elastic scattering and acquired $\langle p_T^2(x_F < 0) \rangle_{el}^{\pi^+}$ (given in Table A1). The next three terms correspond to π^+ mesons which are produced in secondary inelastic interactions of 'primary' π^+ , π^- and π^0 and have occupied the region of $x_F < 0$, acquiring $\langle p_T^2(\pi^+ \rightarrow \pi^+) \rangle_{in}^b$, $\langle p_T^2(\pi^- \rightarrow \pi^+) \rangle_{in}^b$ and $\langle p_T^2(\pi^0 \rightarrow \pi^+) \rangle_{in}^b$, respectively. The latters are free parameters. Their values adopted for this study are presented in Table A2. The next six terms concerns non-identified protons (with $p_p > 0.6$ GeV/c) originating from the elastic πp scattering of pions with $x_F > 0$ and $x_F < 0$, as a result of which the proton acquires $\langle p_T^2(\pi^+ p) \rangle_{el}^f$, $\langle p_T^2(\pi^- p) \rangle_{el}^f$, $\langle p_T^2(\pi^0 p) \rangle_{el}^f$ and $\langle p_T^2(\pi^+ p) \rangle_{el}^b$, $\langle p_T^2(\pi^- p) \rangle_{el}^b$, $\langle p_T^2(\pi^0 p) \rangle_{el}^b$, respectively. The latters (quoted in Table A2) are extracted from the data on $d\sigma_{el}^{\pi N}/dt$ convoluted with the probability (depending on p_p) of the proton non-identification. The last three terms in (A7) corresponds to non-identified protons, originating from inelastic reactions $\pi N \rightarrow pX$, as a result of which the recoil proton acquires $\langle p_T^2(\pi^+ \rightarrow p) \rangle_{in}$, $\langle p_T^2(\pi^- \rightarrow p) \rangle_{in}$ and $\langle p_T^2(\pi^0 \rightarrow p) \rangle_{in}$ (quoted in Table A2). Due to the lack of data, the latters are assumed to be a simple average: $\langle p_T^2(\pi \rightarrow p) \rangle_{in} = (\langle p_T^2(\pi \rightarrow \pi^+) \rangle_{in}^b + \langle p_T^2(\pi \rightarrow \pi^-) \rangle_{in}^b + \langle p_T^2(\pi p) \rangle_{el})/3$. Similar equations can be written down for $\langle p_T^2(x_F > 0) \rangle_A^-$ (including all corresponding terms of (A6)) and $\langle p_T^2(x_F < 0) \rangle_A^-$ (including the first five corresponding terms of (A7)). The chosen values of the corresponding free parameters $\langle p_T^2(\pi \rightarrow \pi^-) \rangle_{in}^f$ and $\langle p_T^2(\pi \rightarrow \pi^-) \rangle_{in}^b$ ($\pi \equiv \pi^+, \pi^-, \pi^0$) are given in Table A2.

'Incident' pion	\bar{p}_π (GeV/c)	w_{in}	$\bar{n}(\pi \rightarrow \pi^+)$	$\bar{n}(\pi \rightarrow \pi^-)$	w_{el}	$\langle p_T^2 \rangle_{el}^\pi$ (GeV/c) ²
$4 < W^2 < 9 \text{ GeV}^2$						
$\pi^+(x_F > 0)$	1.7	0.20	1.14	0.42	0.035	0.31
$\pi^-(x_F > 0)$	1.3	0.19	0.35	1.03	0.041	0.25
$\pi^+(x_F < 0)$	0.71	—	—	—	0.14	0.18
$\pi^-(x_F < 0)$	0.54	—	—	—	0.16	0.16
$9 < W^2 < 25 \text{ GeV}^2$						
$\pi^+(x_F > 0)$	2.9	0.10	1.31	0.48	0.016	0.41
$\pi^-(x_F > 0)$	2.4	0.09	0.52	1.24	0.02	0.37
$\pi^+(x_F < 0)$	0.85	—	—	—	0.07	0.22
$\pi^-(x_F < 0)$	0.68	—	—	—	0.11	0.16

Table A1: The mean momenta \bar{p}_π of pions produced in νN interactions, the probabilities of their inelastic (w_{in}) and elastic (w_{el}) intranuclear interactions, the mean multiplicities $\bar{n}(\pi \rightarrow \pi')$ of secondary pions, and the mean squared transverse momentum $\langle p_T^2 \rangle_{el}^\pi$ (with respect to the weak current axis) acquired by pions undergone elastic πN scattering, at $W^2 < 9 \text{ GeV}^2$ and $W^2 > 9 \text{ GeV}^2$. The corresponding values for π^0 - induced reactions are assumed to be a simple average of those for π^+ and π^- - induced reactions.

Reaction	$W^2 < 9 \text{ GeV}^2$		$W^2 > 9 \text{ GeV}^2$	
	'Incident' momentum	$\langle p_T^2 \rangle$ (GeV/c) ²	'Incident' momentum	$\langle p_T^2 \rangle$ (GeV/c) ²
$\pi^+ N \rightarrow \pi^+(x_F > 0)X$	1.7 GeV/c	0.14	2.9 GeV/c	0.18
$\pi^+ N \rightarrow \pi^-(x_F > 0)X$		0.11		0.12
$\pi^+ N \rightarrow \pi^+(x_F < 0)X$		0.28		0.30
$\pi^+ N \rightarrow \pi^-(x_F < 0)X$		0.15		0.17
$\pi^- N \rightarrow \pi^-(x_F > 0)X$	1.3 GeV/c	0.12	2.4 GeV/c	0.15
$\pi^- N \rightarrow \pi^+(x_F > 0)X$		0.10		0.11
$\pi^- N \rightarrow \pi^-(x_F < 0)X$		0.22		0.24
$\pi^- N \rightarrow \pi^+(x_F < 0)X$		0.12		0.14
$\pi^+ N \rightarrow pX$	1.7 GeV/c	0.30	2.9 GeV/c	0.44
$\pi^- N \rightarrow pX$	1.3 GeV/c	0.22	2.4 GeV/c	0.37
$\pi^+ p \rightarrow \pi^+ p$	1.7 GeV/c	0.47	2.9 GeV/c	0.85
$\pi^- p \rightarrow \pi^- p$	1.3 GeV/c	0.33	2.4 GeV/c	0.71
$\pi^+ p \rightarrow \pi^+ p$	0.71 GeV/c	0.09	0.85 GeV/c	0.10
$\pi^- p \rightarrow \pi^- p$	0.54 GeV/c	0.05	0.68 GeV/c	0.08

Table A2: The values of $\langle p_T^2 \rangle$ (with respect to the weak current axis) acquired by secondary π^\pm mesons with $x_F > 0$ and $x_F < 0$ and non-identified protons in intranuclear inelastic interactions, and by non-identified protons in πp elastic scattering, at $W^2 < 9 \text{ GeV}^2$ and $W^2 > 9 \text{ GeV}^2$. The corresponding values for π^0 - induced reactions are assumed to be a simple average of those for π^+ and π^- - induced reactions.

References

- [1] V.V.Ammosov et al., Fiz. Elem. Chastits At. Yadra **23**, 648, 1992 [Sov. J. Part. Nucl. **23**, 283, 1992]
- [2] N.M.Agababyan et al., YerPhi Preprint-1535(9), 1999, Yerevan
- [3] N.M.Agababyan et al., Yad. Fiz. **65**, 1, 2002 [Phys. of At. Nucl. **65**, 1628, 2002]
- [4] N.M.Agababyan et. al., YerPhi Preprint-1578(3), 2002, Yerevan
- [5] N.M.Agababyan et. al., IHEP Preprint 2002-22, Protvino; Yad. Fiz. (in print)
- [6] D.S.Baranov et al., Z. Phys. C **21**, 197, 1984
- [7] J.Bell et al., Phys. Rev. D **19**, 1, 1979
- [8] T.Kitagaki et al., Phys. Lett. **97B**, 325, 1980
- [9] E.S.Vataga et al., Yad. Fiz. **63**, 1660, 2000
- [10] J.W.Chapman et al., Phys. Rev. D **14**, 14, 1976
- [11] M.Derrick et al., Phys. Rev. D **17**, 1, 1978
- [12] H.Deden et al., Nucl. Phys. B **181**, 375, 1981
- [13] J.J.Aubert et al., Phys. Lett. **95B**, 306, 1980
- [14] P.S.Bosetti et al., Nucl. Phys. B **149**, 13, 1979
- [15] G. Altarelli and G.Martinelli, Phys. Lett. **76B**, 89, 1978
- [16] P.Renton and W.S.C.Williams, Ann. Rev. Nucl. Part. Sci. **31**, 193, 1981
- [17] R.Odorico, Phys. Lett. **89B**, 89, 1979
- [18] P.Mazzanti, R.Odorico and V.Roberto, Phys. Lett. **81B**, 219, 1979
- [19] P.Allen et al., Nucl. Phys. B **188**, 1, 1981
- [20] M.Arneodo et al., (EMC Coll.), Phys. Lett. **149B**, 415, 1984

- [21] M.Arneodo et al., (EMC Coll.), Z. Phys. C **36**, 527, 1987
- [22] M.Z.Akrawy et al., (OPAL Coll.) Z. Phys. C **47**, 505, 1990
- [23] A.Bialas, M.Gyulassy, Nucl. Phys. B **291**, 793, 1987
- [24] B.Andersson et al., Phys. Rep. **97**, 31, 1983
- [25] B.Z.Kopeliovich, Phys. Lett. B **243**, 141, 1990
- [26] A.Airapetian et al., (HERMES Coll.), Eur. Phys. J. C **20**, 479, 2001
- [27] V.Flaminio et al., Compilation CERN-HERA 83-01, 1983
- [28] E.Bracci et al., Compilation CERN-HERA 75-2, 1975
- [29] W.Witteck et al., (BEBC WA59 Coll.), Z. Phys. C **40**, 231, 1988
- [30] P.Bosetti et al., Nucl. Phys. B **54**, 141, 1973
- [31] D.Allasia et al., Nucl. Phys. B **268**, 1, 1986
- [32] V.V.Ammosov et al., Yad. Fiz. **46**, 130, 1987; Sov. J. Nucl. Phys. **46**, 80, 1987

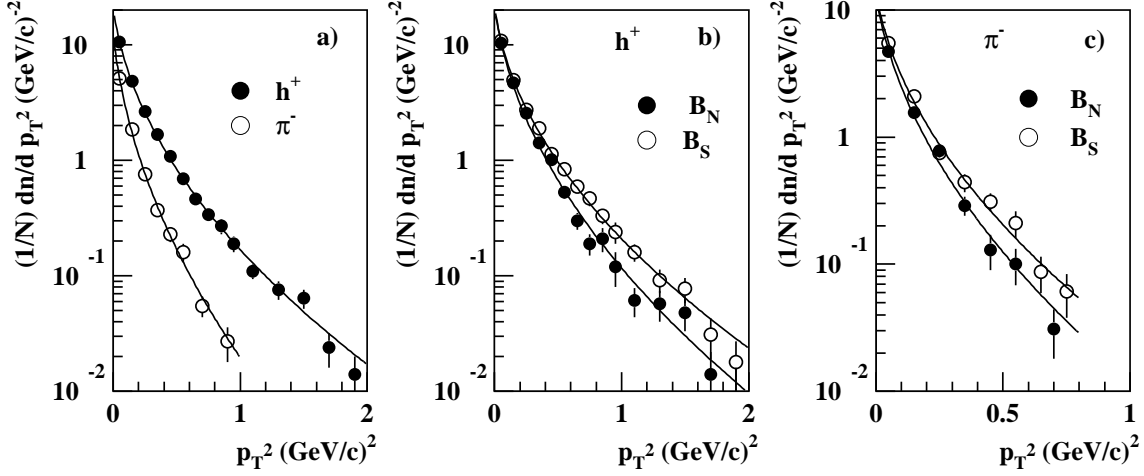


Figure 1: The p_T^2 - distributions of a) h^+ and π^- for the whole event sample, b) h^+ for B_N and B_S subsamples, c) π^- for B_N and B_S subsamples. Lines are results of the fit (see text).

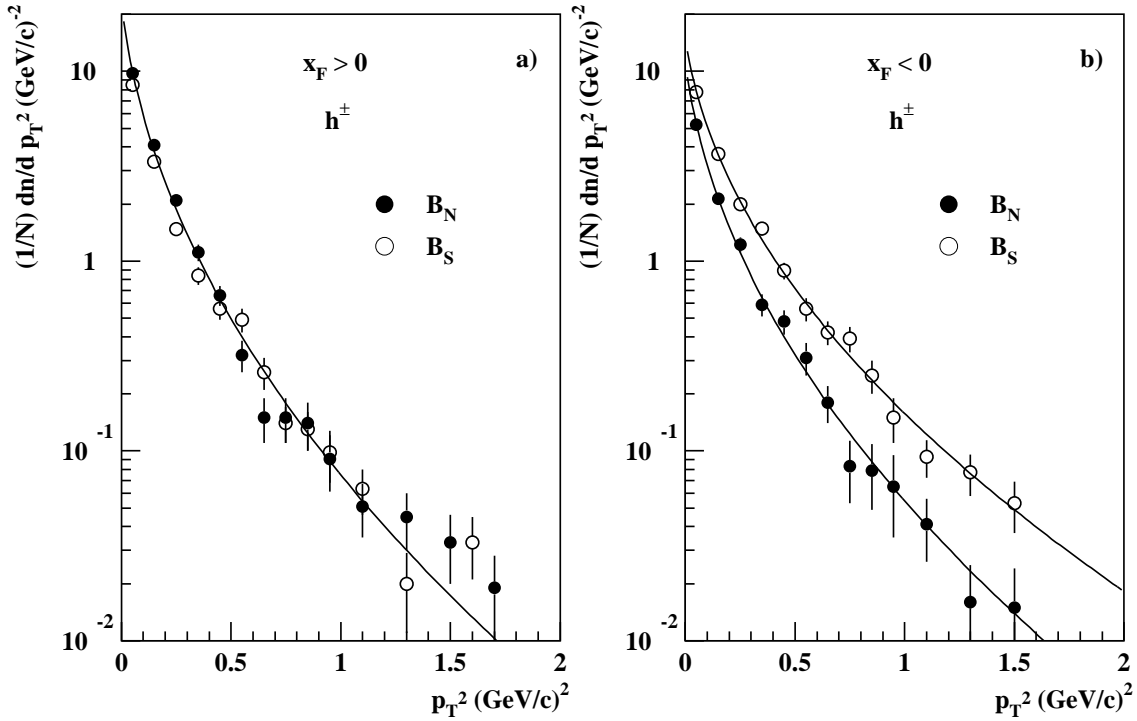


Figure 2: The p_T^2 - distributions of charged hadrons for B_N and B_S subsamples at a) $x_F > 0$ and b) $x_F < 0$. Lines are results of the fit (see text).

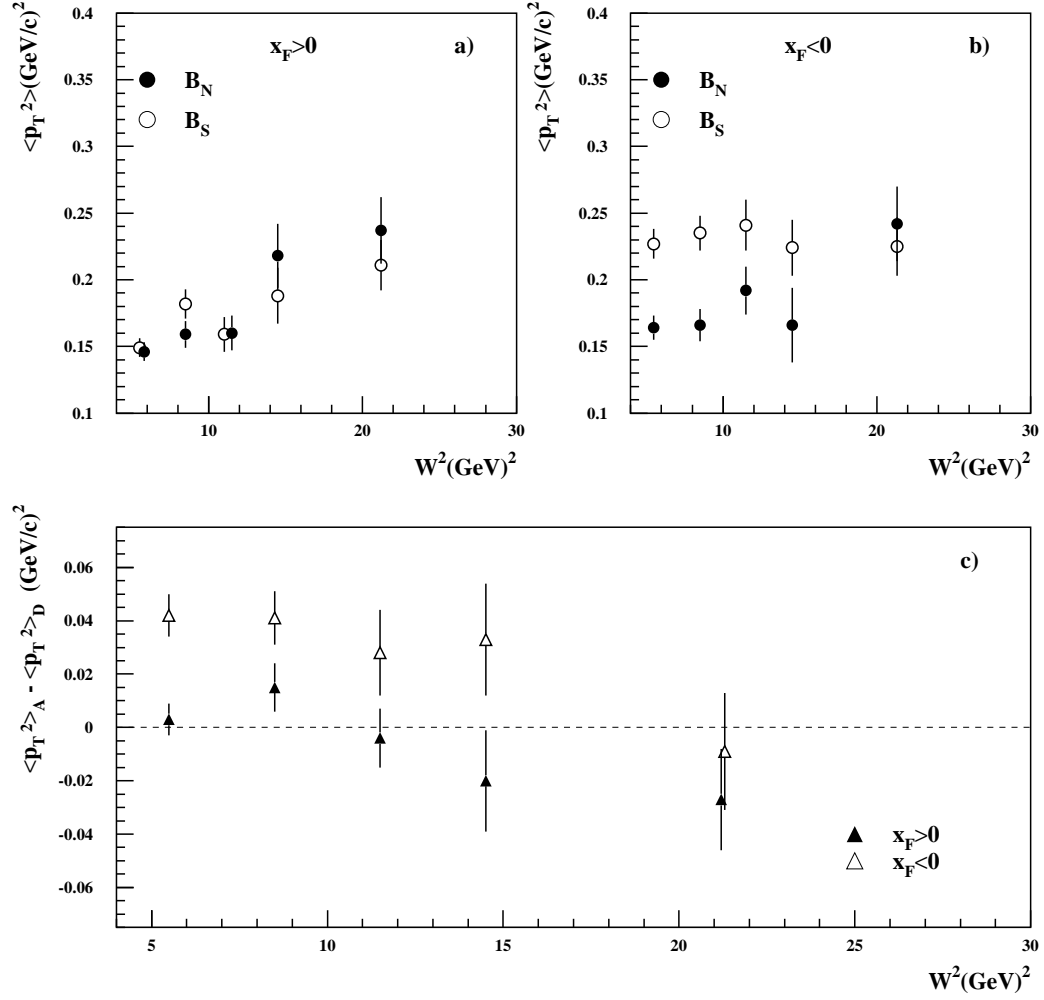


Figure 3: The W^2 -dependence of a) $\langle p_T^2 \rangle$ at $x_F > 0$ for B_N and B_S subsamples, b) $\langle p_T^2 \rangle$ at $x_F < 0$ for B_N and B_S subsamples, c) the difference $\langle p_T^2 \rangle_A - \langle p_T^2 \rangle_D$.

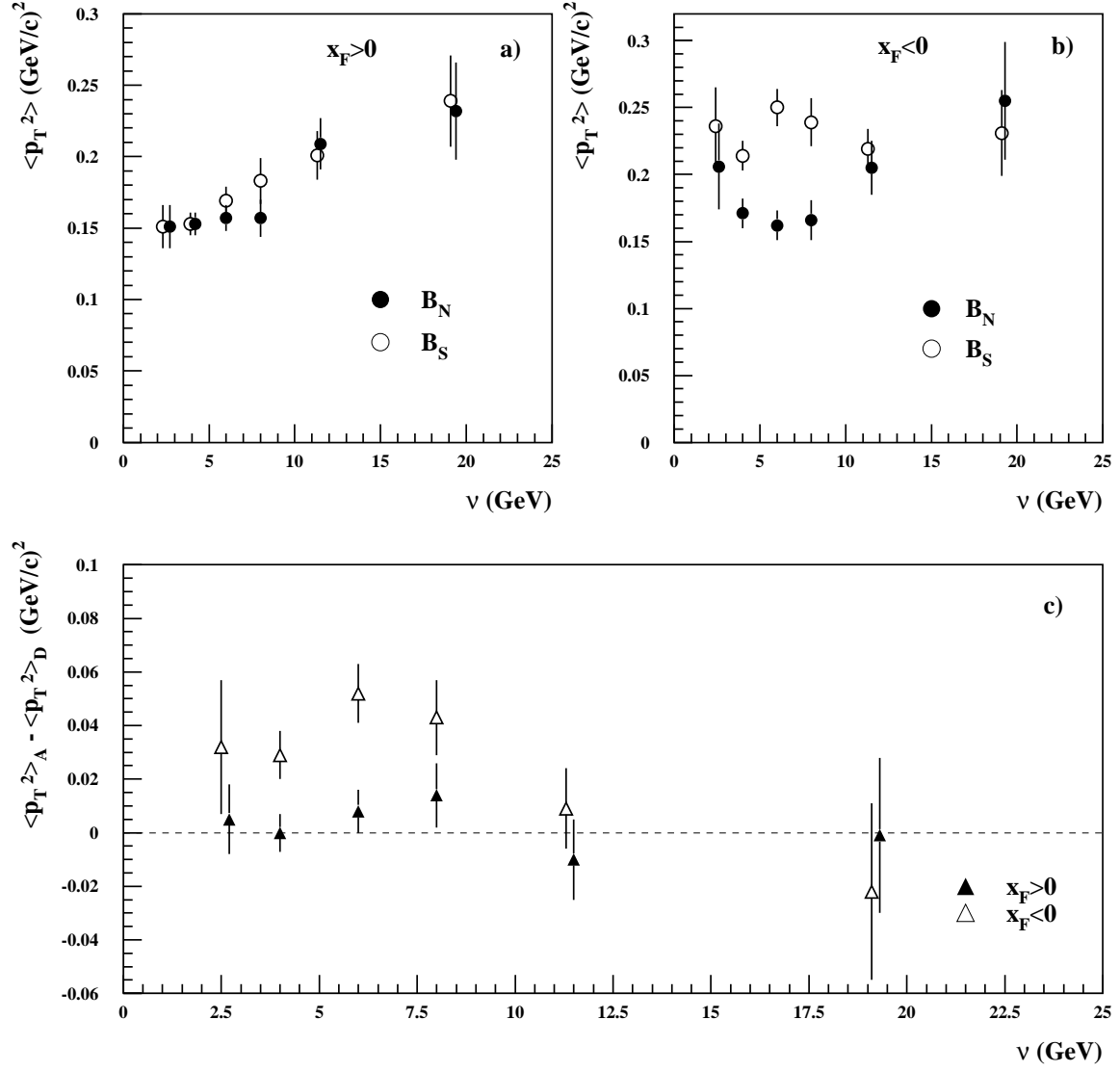


Figure 4: The ν -dependence of a) $\langle p_T^2 \rangle$ at $x_F > 0$ for B_N and B_S subsamples, b) $\langle p_T^2 \rangle$ at $x_F < 0$ for B_N and B_S subsamples, c) the difference $\langle p_T^2 \rangle_A - \langle p_T^2 \rangle_D$.

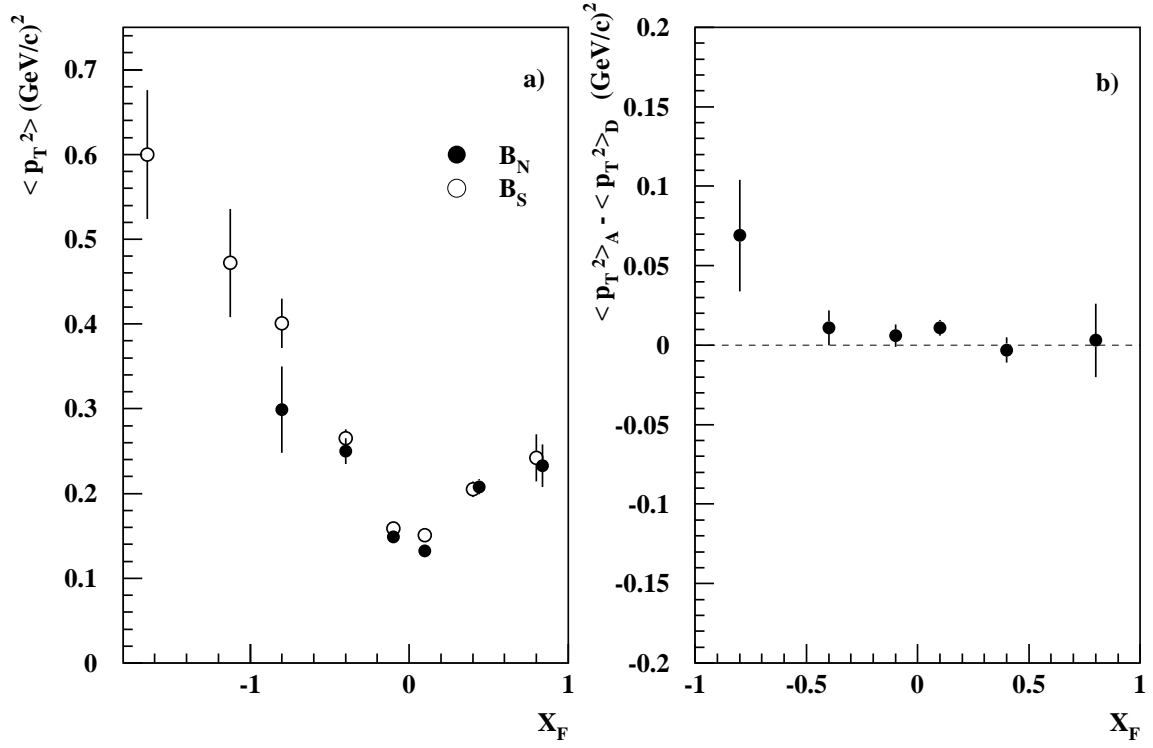


Figure 5: The x_F - dependence of a) $\langle p_T^2 \rangle$ for B_N and B_S subsamples, b) the difference $\langle p_T^2 \rangle_A - \langle p_T^2 \rangle_D$.

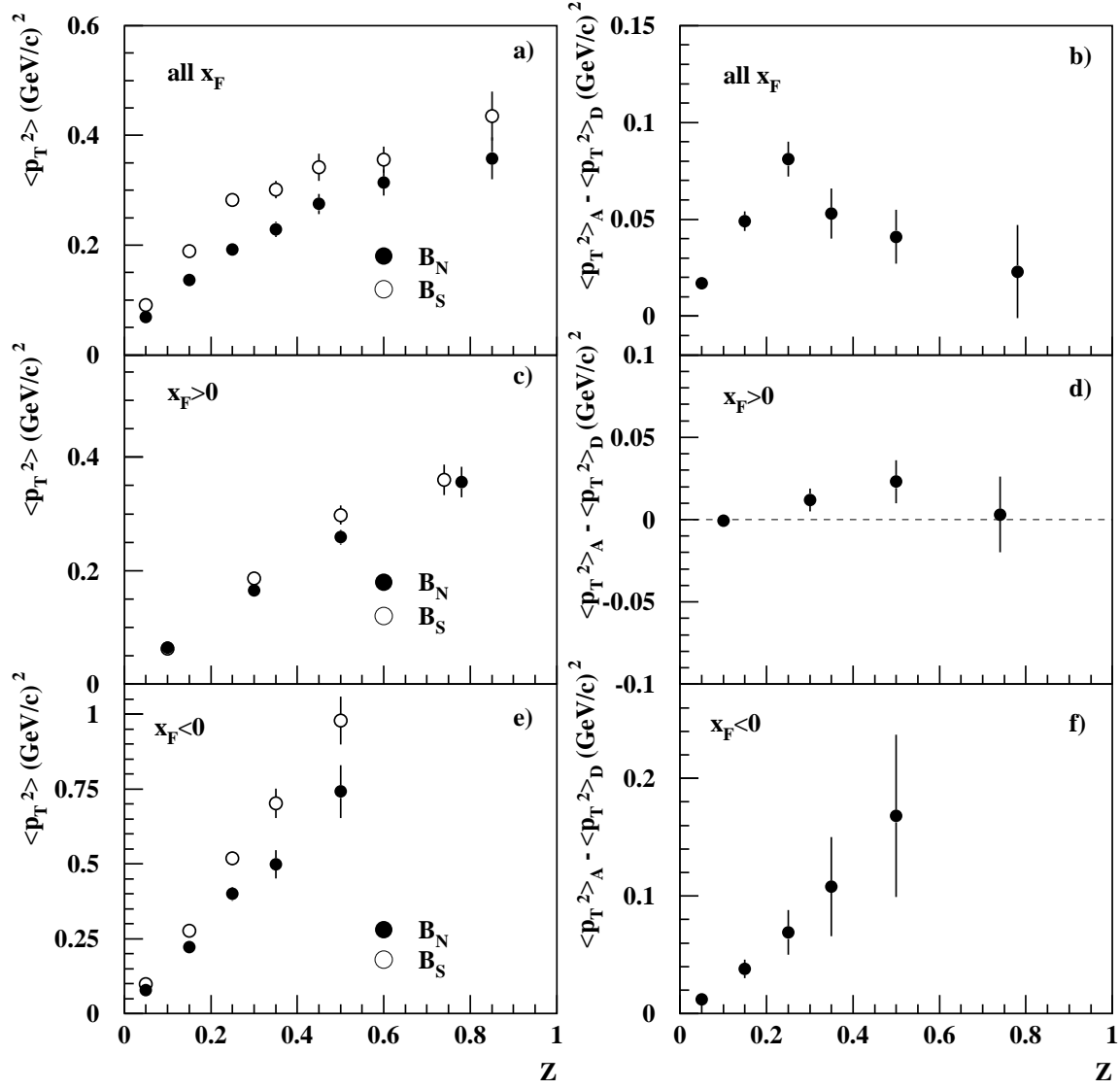


Figure 6: The z -dependence of $\langle p_T^2 \rangle$ for B_N and B_S subsamples (a, c, e) and of the difference $\langle p_T^2 \rangle_A - \langle p_T^2 \rangle_D$ (b, d, f).

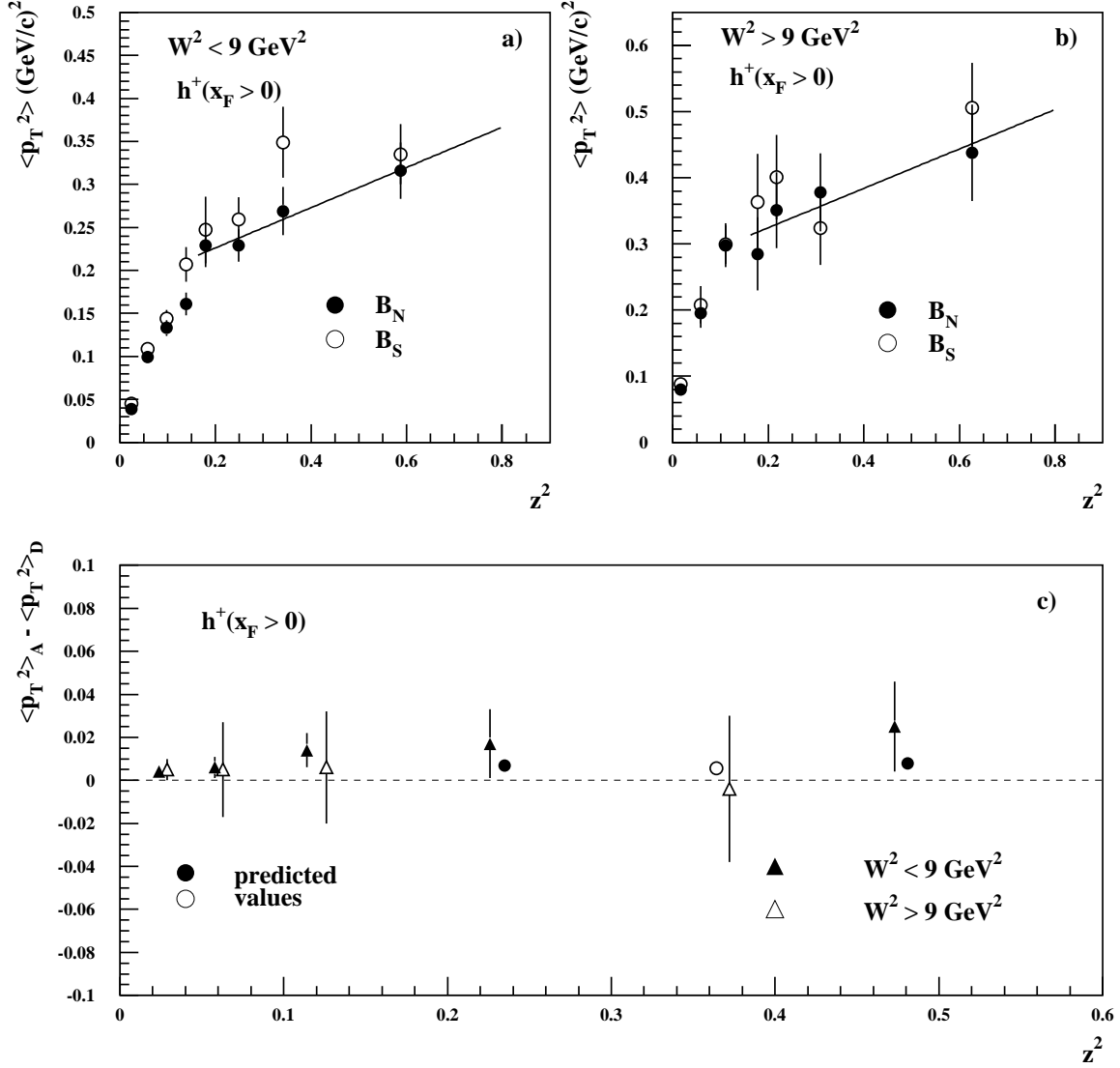


Figure 7: The z^2 -dependence of: $\langle p_T^2 \rangle$ of positively charged hadrons with $x_F > 0$ a) at $W^2 < 9 \text{ GeV}^2$ and b) $W^2 > 9 \text{ GeV}^2$; c) the difference $\langle p_T^2 \rangle_A - \langle p_T^2 \rangle_D$. The lines in Figs. 7a and 7b are the fit results (see text).